

Two Strings with a Dynamic Interior Mass: A Feedback Control Design with Guaranteed Exponential Decay

Zoe Brown and Ahmet Özkan Özer

Abstract—This paper investigates the exponential stabilization of a coupled two-string system joined by a dynamic interior mass. The combined effect of three feedback mechanisms, boundary damping from tip velocity, higher-order nodal damping from angular velocity, and lower-order nodal damping from mass velocity, is analyzed using a Lyapunov framework. Exponential stability is established unconditionally, without constraints on wave speeds or mass location, improving upon earlier results that lower-order nodal damping, as in Hansen-Zuazua’95, or boundary damping alone, as in Lee-You’89, does not ensure exponential decay without additional structural conditions. Moreover, the lower-order feedback can be removed without loss of exponential decay when combined with the other two mechanisms, via a compact perturbation argument. These results apply to hybrid systems with interior or tip mass interfaces, including overhead cranes, deep-sea cables, and fluid structure interaction. Theoretical findings are validated through numerical simulations.

Index Terms—Serially-connected strings, Hybrid PDE–ODE systems, Boundary and interface feedback control, Interior-mass dynamics, Unconditional exponential stability

I. INTRODUCTION

Hybrid PDE–ODE systems arise in many engineering applications, including overhead cranes with flexible cables [1], deep sea cables with tip dynamics [2], bridge cables with internal or external dampers [3], and fluid–structure interaction systems [4]. These systems often involve interior masses or joints, leading to complex transmission conditions and requiring tailored damping strategies. Recent engineering studies have proposed passive or active mass–spring–damper devices for vibration suppression and energy dissipation in such systems. Applications include overhead transmission lines [5], robotic manipulators [6], underwater cables [7], and bridge cables [3], where point masses serve as absorbers or actuators under active or semi-active control. Beyond classical devices such as Stockbridge dampers, newer approaches incorporate smart materials like piezoelectric and magnetostrictive elements to provide tunable impedance and feedback at interior or boundary locations [8].

This paper investigates one such configuration, focusing on the stabilizing effect of boundary and interface feedback controls. We study a serially-connected system of two non-homogeneous strings joined by a point mass $m > 0$. The dynamics are governed by wave equations modeling transverse vibrations over (l_0, l_1) and (l_1, l_2) , with $l_0 = 0$. The interface at $x = l_1$ introduces interior mass dynamics via an inertial

term from $m > 0$, coupling the two string segments (see Fig. 1). Key parameters include mass densities ρ_i and stiffness coefficients α_i for each segment ($i = 1, 2$). We prove that the system achieves unconditional exponential stability using a Lyapunov-based approach.

The displacement fields of the two strings are denoted by $w^i(x, t)$ for $i = 1, 2$. At the coupling interface $x = l_1$, displacement continuity is enforced through a shared dynamic variable $z(t) := w^1(l_1, t) = w^2(l_1, t)$, representing the displacement of the point mass. Let $g_1(t)$ and $g_2(t)$ be the control inputs at the interface $x = l_1$ and the free end $x = l_2$, respectively. The governing equations are given by

$$\{\rho_i w_{tt}^i - \alpha_i w_{xx}^i(x, t) = 0, \quad (x, t) \in (l_{i-1}, l_i) \times \mathbb{R}^+, \quad (1)$$

$$\begin{cases} w^1(0, t) = 0, \\ w^1(l_1, t) = w^2(l_1, t) = z(t), \\ \alpha_1 w_x^1(l_1, t) - \alpha_2 w_x^2(l_1, t) + m z_{tt}(t) = g_1(t), \\ w_x^2(l_2, t) = g_2(t), \end{cases} \quad (2)$$

$$\{(w^i, w_t^i)(x, 0) = (w_0^i, w_1^i)(x), \quad x \in [l_{i-1}, l_i], i = 1, 2. \quad (3)$$

The control inputs are subsequently chosen in the form of feedback laws as defined below

$$\begin{cases} g_1(t) := -b_0 (\alpha_1 w_{xt}^1(l_1, t) - \alpha_2 w_{xt}^2(l_1, t)) - b_1 w_t^1(l_1, t), \\ g_2(t) := -d_1 w_t^2(l_2, t). \end{cases} \quad (4)$$

Specifically, $g_1(t)$ combines higher-order slope-velocity feedback and lower-order interface-velocity feedback at $x = l_1$, while $g_2(t)$ applies lower-order velocity feedback at the free end $x = l_2$. The gains $b_0 > 0$ and $b_1 > 0$ correspond to slope-difference and velocity damping at the interface, respectively, and $d_1 > 0$ denotes boundary damping at the right end. These feedbacks are central to the system’s stabilization, as analyzed in the next sections.

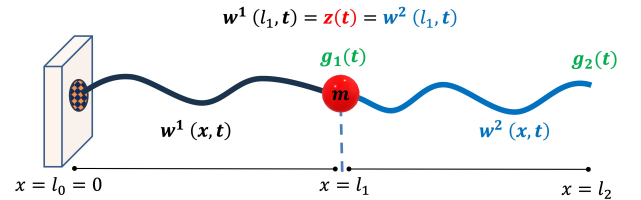


Fig. 1: Schematic of two coupled strings connected by an interior mass m at $x = l_1$. Control inputs $g_1(t)$ and $g_2(t)$ act at the interface and the right boundary, respectively.

We introduce an auxiliary dynamic variable $\eta(t)$ by

$$\eta(t) := b_0 (\alpha_1 w_x^1(l_1, t) - \alpha_2 w_x^2(l_1, t)) + m z_t(t), \quad (5)$$

*The second author acknowledges the support of the Fulbright U.S. Scholar Program under the 2024-2025 Research Award to conduct research in France.

Department of Mathematics, Western Kentucky University (WKU), Bowling Green, KY 42101, USA. Email: ozkan.ozer@wku.edu

By differentiating (5) and using the transmission condition in (2), $\eta(t)$ satisfies the initial-value problem

$$\begin{cases} \eta_t(t) = -(\alpha_1 w_x^1 - \alpha_2 w_x^2)(l_1, t) - b_1 z_t(t), t \in \mathbb{R}^+, \\ \eta(0) = \eta_0 := b_0(\alpha_1 w_x^1 - \alpha_2 w_x^2)(l_1, 0) + m z_t(0). \end{cases} \quad (6)$$

A. Literature on the PDE Model and Stability Results

The stabilization of hyperbolic systems with interior point masses has been widely studied. Early works such as [9], [10] introduced hybrid string models, showing that interior masses prevent strong stability when only velocity-type feedback is applied at the joint ($x = 0$), i.e., when $b_0, d_1 \equiv 0, b_1 \neq 0$ in (4). If a velocity-type boundary feedback is applied only at the right boundary ($x = \ell_2$), i.e., $b_0, b_1 \equiv 0, d_1 \neq 0$, the system attains strong stability but lacks uniform exponential decay, as eigenvalues cluster near the imaginary axis [11]. Further analysis in [12] showed that in such cases, only polynomial decay—typically at rate t^{-1} —can be achieved due to the lack of sufficient dissipation.

Subsequent studies, including [4], [13], [14], [15], [16], extended these ideas to more intricate geometries such as networks, trees, and fluid–structure interaction models, often featuring transmission conditions through interior masses or junctions. These works primarily employed lower-order nodal or boundary damping and demonstrated that stabilization depends sensitively on system parameters, interface locations, and controller placement. While strong or polynomial stability can often be achieved under specific configurations, such damping strategies alone generally fail to ensure uniform exponential stabilization.

A key advance appeared in [17], [18], which introduced higher-order (angular velocity) damping for strings with tip masses and established exponential stability via Lyapunov methods and spectral analysis. This marked a shift in control design, showing that higher-order feedback can succeed where lower-order damping fails. Although our approach does not rely on backstepping, we note that backstepping-based boundary control, as introduced in [19], provides a general framework for PDE and PDE–ODE stabilization and is complementary to higher-order strategies. Related work on PDE–ODE–PDE systems, such as deep-sea cables with tip actuators [2], further highlights the effectiveness of boundary-based higher-order feedback.

B. Our Motivation and Major Results

As shown in [9], [10], [11], [12], neither exponential nor strong stability is guaranteed when using only boundary damping at $x = l_2$ or lower-order damping at the mass interface $x = l_1$. Building on the higher-order feedback approach of [17], we develop a new stabilization framework that combines higher- and lower-order damping at the mass with boundary damping at the free end.

We establish unconditional exponential stability via a Lyapunov-based approach under the assumption that b_0, b_1 , and d_1 are positive. Unlike previous works with $b_0 \equiv 0$ in (4), our model includes higher-order angular velocity feedback at the mass, which plays a decisive role in stabilization.

Remarkably, we show that the lower-order damping b_1 can be omitted without loss of exponential decay by treating the reduced system as a compact perturbation. This highlights the spectral dominance of higher-order damping and enables a more efficient design.

The proposed strategy is robust concerning wave speeds, damping strengths, and mass location, and does not rely on structural compatibility conditions, an improvement over earlier results.

The remainder of the paper is organized as follows. Section II establishes well-posedness via a first-order reformulation. Section III presents the main exponential stability results. Section IV introduces a finite difference scheme preserving the decay rate and provides numerical simulations validating the theory.

II. WELL-POSEDNESS

To analyze the stability of the system (1)–(3), we define the total energy $E(t)$ as

$$\begin{aligned} E(t) = & \frac{1}{2} \sum_{j=1}^2 \int_{l_{j-1}}^{l_j} \left[\rho_j (w_t^j(x, t))^2 + \alpha_j (w_x^j(x, t))^2 \right] dx \\ & + \frac{1}{2} \frac{(\eta(t))^2}{m + b_0 b_1}. \end{aligned} \quad (7)$$

Lemma 1. *For all $t \geq 0$, the energy is dissipative,*

$$\begin{aligned} \frac{dE(t)}{dt} = & -\frac{b_0}{m + b_0 b_1} [\alpha_1 w_x^1 - \alpha_2 w_x^2]^2(l_1, t) \\ & - \frac{m b_1}{m + b_0 b_1} (z_t(t))^2 - d^1 (w_t^2)^2(l_2, t). \end{aligned} \quad (8)$$

Proof. We differentiate (7) along with (1)–(5):

$$\begin{aligned} \frac{dE(t)}{dt} = & \sum_{j=1}^2 \int_{l_{j-1}}^{l_j} \rho_j (w_t^j(x, t)) (w_{tt}^j(x, t)) dx \\ & + \sum_{j=1}^2 \int_{l_{j-1}}^{l_j} \alpha_j (w_x^j(x, t)) (w_{xt}^j(x, t)) dx + \frac{\eta(t) \eta_t(t)}{m + b_0 b_1} \\ = & \sum_{j=1}^2 \alpha_j (w_t^j(x, t)) (w_x^j(x, t)) \Big|_{l_{j-1}}^{l_j} + \frac{\eta(t) \eta_t(t)}{m + b_0 b_1} \\ = & -d_1 (w_t^2)^2(l_2, t) - \alpha_2 (w_t^2 w_x^2)(l_1, t) + \alpha_1 (w_t^1 w_x^1)(l_1, t) \\ & + \frac{(b_0(\alpha_1 w_x^1 - \alpha_2 w_x^2)(l_1, t) + m z_t(t))(-(\alpha_1 w_x^1 - \alpha_2 w_x^2)(l_1, t) - b_1 z_t(t))}{m + b_0 b_1}. \end{aligned}$$

Using $z(t) = w^1(l_1, t) = w^2(l_1, t)$ and simplifying yields the dissipation identity (8). \square

Let $H_L^1(0, l_1) = \{f \in H^1(0, l_1) : f(l_1) = 0\}$. Now, define the energy space \mathcal{H} by $\mathcal{H} = H_L^1(0, l_1) \times L^2(0, l_1) \times H^1(l_1, l_2) \times L^2(l_1, l_2) \times \mathbb{C}$ equipped with the inner product

$$\begin{aligned} \langle U, \tilde{U} \rangle_{\mathcal{H}} = & \sum_{j=1}^2 \int_{l_{j-1}}^{l_j} [\rho_j (p^j \bar{p}^j) + \alpha_j (u_x^j \bar{u}_x^j)](x, t) dx \\ & + \frac{\theta \bar{\theta}}{m + b_0 b_1} \end{aligned}$$

for $U = (u^1, p^1, u^2, p^2, \theta)$, $\tilde{U} = (\tilde{u}^1, \tilde{p}^1, \tilde{u}^2, \tilde{p}^2, \tilde{\theta}) \in \mathcal{H}$. The norm induced by the inner product is $\|U\|_{\mathcal{H}}^2 := \langle U, U \rangle_{\mathcal{H}}$. Introducing $w_t^1 = v^1$ and $w_t^2 = v^2$, the system (1)–(3) can be recast as the first-order initial value problem

$$\frac{d}{dt} U(t) = \mathcal{A} U(t), \quad U(0) = U_0, \quad \forall t > 0, \quad (9)$$

where $U = (w^1, v^1, w^2, v^2, \eta)^\top$ and $U_0 = (w_0^1, w_1^1, w_0^2, w_1^2, \eta_0)^\top$. The operator $\mathcal{A} : \mathcal{D}(\mathcal{A}) \subset \mathcal{H} \rightarrow \mathcal{H}$ is defined by

$$\mathcal{A}[w^1, v^1, w^2, v^2, \eta]^\top = [v^1, \frac{\alpha_1}{\rho_1} w_{xx}^1, v^2, \frac{\alpha_2}{\rho_2} w_{xx}^2, -(w_x^1 - w_x^2)(l_1) - b_1 v^1(l_1)]^\top.$$

with domain

$$\mathcal{D}(\mathcal{A}) = \{U \in \mathcal{H} : w^1 \in (H_L^1 \cap H^2)(0, l_1), w^2 \in H^2(l_1, l_2), v^1 \in H_L^1(0, l_1), v^2 \in H^1(l_1, l_2), \alpha_2 w_x^2(l_2) = -d_1 v^2(l_2), b_0(\alpha_1 w_x^1(l_1) - \alpha_2 w_x^2(l_1)) + m v^1(l_1) = \eta\}.$$

If $(w^1, v^1, w^2, v^2, \eta)$ is a sufficiently regular solution of (1)–(3), then it satisfies the abstract Cauchy problem

$$U_t = \mathcal{A}U, \quad U(0) = U_0, \quad (10)$$

in the Hilbert space \mathcal{H} . where $U = (w^1, v^1, w^2, v^2, \eta)$ and $U_0 = (w_0^1, w_1^1, w_0^2, w_1^2, \eta_0)$. A direct computation yields

$$\operatorname{Re}(\mathcal{A}U, U)_{\mathcal{H}} = -\frac{b_0}{m+b_0b_1} |(\alpha_1 w_x^1 - \alpha_2 w_x^2)(l_1)|^2 - \frac{mb_1}{m+b_0b_1} |v^1(l_1)|^2 - d_1 |v^2(l_2)|^2,$$

showing that \mathcal{A} is dissipative. To prove m -dissipativity, let $F = (f_1, f_2, f_3, f_4, f_5) \in \mathcal{H}$ be given. By the Lax–Milgram Theorem, there exists a unique $U \in \mathcal{D}(\mathcal{A})$ solving $-\mathcal{A}U = F$. Thus, \mathcal{A} is m -dissipative and $0 \in \rho(\mathcal{A})$.

By the Lumer–Phillips Theorem, \mathcal{A} generates a C_0 -semigroup of contractions $(e^{t\mathcal{A}})_{t \geq 0}$ on \mathcal{H} , and the solution to (10) is given by $(e^{t\mathcal{A}})_{t \geq 0}$ establishing the well-posedness of the system.

Theorem 2. *Letting $U_0 \in \mathcal{H}$, the system (10) admits a unique weak solution U satisfying $U \in C^0(\mathbb{R}_+, \mathcal{H})$.*

Moreover, if $U_0 \in D(\mathcal{A})$, the system (10) admits a unique strong solution U satisfying $U \in C^1(\mathbb{R}_+, \mathcal{H}) \cap C^0(\mathbb{R}_+, D(\mathcal{A}))$.

III. EXPONENTIAL STABILITY RESULTS

For $\epsilon_1, \epsilon_2 > 0$, we define the Lyapunov function $L(t)$ as

$$\begin{aligned} L(t) &:= E(t) + \epsilon_1 I_1(t) + \epsilon_2 I_2(t), \\ V(t) &:= tL(t) + P_1(t) + P_2(t), \end{aligned} \quad (11)$$

where the auxiliary functionals $I_j(t)$ and $P_j(t)$, for $j = 1, 2$, are defined by

$$\begin{aligned} I_j(t) &:= 2 \int_{l_{j-1}}^{l_j} \rho_j w_t^j(x, t) w_x^j(x, t) dx, \\ P_j(t) &:= 3 \int_{l_{j-1}}^{l_j} (x - l_{j-1}) \rho_j w_x^j(x, t) w_t^j(x, t) dx. \end{aligned}$$

Lemma 3. *Let $C := \max_{j=1,2} \sqrt{\frac{\rho_j}{\alpha_j}}$ and $\epsilon := \max_{j=1,2} \epsilon_j$. Then, for any $0 < \epsilon < \frac{1}{2C}$, $L(t)$ defined in (11) satisfies*

$$(1 - 2\epsilon C)E(t) \leq L(t) \leq (1 + 2\epsilon C)E(t). \quad (12)$$

Proof. For each $j = 1, 2$, we apply Young's inequality to estimate the cross term in $I_j(t)$:

$$|I_j(t)| \leq \sqrt{\frac{\rho_j}{\alpha_j}} \int_{l_{j-1}}^{l_j} [\rho_j (w_t^j)^2(x, t) + \alpha_j (w_x^j)^2(x, t)] dx.$$

Summing over $j = 1, 2$ and recalling the definition of $L(t)$, the desired estimate follows immediately. \square

Lemma 4. *Let $C_1 := 3 \max_{j=1,2} \left((l_j - l_{j-1}) \sqrt{\frac{\rho_j}{\alpha_j}} \right) > 0$, and define $C_2 := \frac{C_1}{1-2\epsilon C}$. Then for any $0 < \epsilon < \frac{1}{2C}$, the functional $V(t)$ defined in (11) satisfies*

$$(t - C_2)L(t) \leq V(t) \leq (t + C_2)L(t), \quad \forall t \geq 0.$$

Proof. By Young's inequality, we estimate each $P_j(t)$ term as follows

$$\begin{aligned} |P_1(t)| &\leq \frac{3l_1}{2} \sqrt{\frac{\rho_1}{\alpha_1}} \int_{l_0}^{l_1} (\rho_1 (w_t^1)^2 + \alpha_1 (w_x^1)^2) dx, \\ |P_2(t)| &\leq \frac{3(l_2 - l_1)}{2} \sqrt{\frac{\rho_2}{\alpha_2}} \sum_{j=1}^2 \int_{l_1}^{l_j} (\rho_2 (w_t^2)^2 + \alpha_2 (w_x^2)^2) dx. \end{aligned}$$

Summing the two estimates yields $|P_1(t) + P_2(t)| \leq C_1 E(t) \leq \frac{C_1}{1-2\epsilon C} L(t)$, where the second inequality uses Lemma 3, completing the proof of Lemma 4. \square

Lemma 5. *The Lyapunov functional $L(t)$ defined in (11) satisfies $\frac{dL(t)}{dt} \leq 0$ provided that the feedback gains $b_0, b_1, d_1 > 0$ and the positive parameters δ, ϵ_1 , and ϵ_2 satisfy the following conditions*

$$\begin{aligned} \epsilon_2 &\leq \min \left(\frac{1}{2C}, \frac{\alpha_2 d_1}{d_1^2 + \alpha_2 \rho_2} \right), \\ \epsilon_1 &\leq \min \left(\frac{1}{2C}, \frac{\epsilon_2 b_0 \alpha_1}{b_0 \alpha_2 + \epsilon_2 (m + b_0 b_1)}, \frac{m b_1}{\rho_1 (m + b_0 b_1)} \right), \\ \frac{b_0 \alpha_1}{b_0 \alpha_2 + (m + b_0 b_1) \epsilon_2} &< \delta < \frac{b_0 \alpha_1 - (m + b_0 b_1) \epsilon_1}{b_0 \alpha_2}. \end{aligned} \quad (13)$$

Proof. For $j = 1, 2$, differentiating $I_j(t)$ along the solutions of (1)–(3) yields

$$\begin{aligned} \frac{dI_j(t)}{dt} &= 2 \int_{l_{j-1}}^{l_j} \alpha_j w_{xx}^j w_x^j dx + 2 \int_{l_{j-1}}^{l_j} \rho_j w_t^j w_{xt}^j dx \\ &= \left[\alpha_j (w_x^j)^2 + \rho_j (w_t^j)^2 \right]_{l_{j-1}}^{l_j}. \end{aligned} \quad (14)$$

Summing over j and simplifying

$$\begin{aligned} \sum_{j=1}^2 \epsilon_j \frac{dI_j(t)}{dt} &\leq \epsilon_2 \left(\frac{d_1^2}{\alpha_2} + \rho_2 \right) (w_t^2)^2(l_2) \\ &\quad + (\alpha_1 \epsilon_1 (w_x^1)^2 - \alpha_2 \epsilon_2 (w_x^2)^2)(l_1) + \epsilon_1 \rho_1 (z_t)^2. \end{aligned} \quad (15)$$

Using this and Lemma 1, the derivative of $L(t)$ becomes

$$\begin{aligned} \frac{dL(t)}{dt} &= -\frac{b_0}{m + b_0 b_1} [\alpha_1 w_x^1 - \alpha_2 w_x^2]^2(l_1) \\ &\quad - \left[\frac{m b_1}{m + b_0 b_1} - \epsilon_1 \rho_1 \right] (z_t)^2 \\ &\quad - \left[d_1 - \epsilon_2 \left(\frac{d_1^2}{\alpha_2} + \rho_2 \right) \right] (w_t^2)^2(l_2) \\ &\quad + (\alpha_1 \epsilon_1 (w_x^1)^2 - \alpha_2 \epsilon_2 (w_x^2)^2)(l_1). \end{aligned} \quad (16)$$

We now expand the interface term via the identity $[\alpha_1 w_x^1 - \alpha_2 w_x^2]^2 \geq (\alpha_1)^2 (w_x^1)^2 + (\alpha_2)^2 (w_x^2)^2 - \delta \alpha_1 \alpha_2 (w_x^1)^2 - \frac{1}{\delta} \alpha_1 \alpha_2 (w_x^2)^2$. Inserting this into (16) gives

$$\begin{aligned} \frac{dL(t)}{dt} \leq & - \left[\frac{b_0(\alpha_1)^2}{m+b_0b_1} - \alpha_1\epsilon_1 - \frac{\delta b_0\alpha_1\alpha_2}{m+b_0b_1} \right] (w_x^1)^2(l_1) \\ & - \left[\frac{b_0(\alpha_2)^2}{m+b_0b_1} + \alpha_2\epsilon_2 - \frac{b_0\alpha_1\alpha_2}{\delta(m+b_0b_1)} \right] (w_x^2)^2(l_1) \\ & - \left[\frac{mb_1}{m+b_0b_1} - \epsilon_1\rho_1 \right] (z_t)^2 - \left[d_1 - \epsilon_2 \frac{d_1^2 + \alpha_2\rho_2}{\alpha_2} \right] (w_t^2)^2(l_2). \end{aligned}$$

Each bracket is nonnegative under (13), so $\frac{dL(t)}{dt} \leq 0$. \square

Theorem 6. Let the parameters $\delta, \epsilon_1, \epsilon_2 > 0$ satisfy

$$\begin{cases} \epsilon_2 \leq \min \left(\frac{1}{2C}, \sqrt{\frac{\alpha_2}{\rho_2}}, \frac{\alpha_2 d_1}{d_1^2 + \alpha_2 \rho_2} \right), \\ \epsilon_1 \leq \min \left(\frac{1}{2C}, \sqrt{\frac{\alpha_1}{\rho_1}}, \right. \\ \left. \frac{\epsilon_2 b_0 \alpha_1}{b_0 \alpha_2 + \epsilon_2(m+b_0b_1)}, \frac{mb_1}{\rho_1(m+b_0b_1)} \right), \\ \frac{b_0 \alpha_1}{b_0 \alpha_2 + (m+b_0b_1)\epsilon_2} < \delta < \frac{b_0 \alpha_1 - (m+b_0b_1)\epsilon_1}{b_0 \alpha_2}. \end{cases} \quad (17)$$

Then, there exists a time $T > \max(T_1, T_2, T_3, T_4)$ such that $\frac{dV(t)}{dt} \leq 0$ for all $t \geq T$, where

$$\begin{aligned} T_1 &:= \frac{\frac{3}{2}\alpha_1 l_1(m+b_0b_1) + 2b_0^2\alpha_1^2}{b_0\alpha_1^2 - \alpha_1\epsilon_1(m+b_0b_1) - \delta b_0\alpha_1\alpha_2}, \\ T_2 &:= \frac{\frac{3}{2}\alpha_2(l_2-l_1)(m+b_0b_1) + 2b_0^2\alpha_2^2}{b_0\alpha_2^2 + \alpha_2\epsilon_2(m+b_0b_1) - \frac{b_0\alpha_1\alpha_2}{\delta}}, \\ T_3 &:= \frac{\frac{3}{2}\rho_1 l_1(m+b_0b_1) + m^2}{mb_1 - \epsilon_1\rho_1(m+b_0b_1)}, T_4 := \frac{\frac{3}{2}(l_2-l_1)\rho_2\alpha_2}{\alpha_2 d_1 - \epsilon_2(d_1^2 + \alpha_2\rho_2)}. \end{aligned}$$

Proof. For each $j = 1, 2$, we compute $\frac{d}{dt} P_j(t)$ by differentiating and integrating by parts

$$\begin{aligned} \frac{dP_j(t)}{dt} &= \frac{3}{2}(l_j - l_{j-1}) \left[\rho_j (w_t^j(l_j, t))^2 + \alpha_j (w_x^j(l_j, t))^2 \right] \\ &\quad - \frac{3}{2} \int_{l_{j-1}}^{l_j} \left[\rho_j (w_t^j)^2 + \alpha_j (w_x^j)^2 \right] dx. \end{aligned}$$

Combining this with the Lyapunov structure, and using $\epsilon_1 < \sqrt{\frac{\alpha_1}{\rho_1}}$ and $\epsilon_2 < \sqrt{\frac{\alpha_2}{\rho_2}}$, we estimate

$$\begin{aligned} \frac{dV(t)}{dt} &= \frac{1}{2} \sum_{j=1}^2 \int_{l_{j-1}}^{l_j} \left[\rho_j (w_t^j)^2 + \alpha_j (w_x^j)^2 \right] dx \\ &\quad + \frac{1}{2(m+b_0b_1)} \eta(t)^2 + \epsilon_1 I_1(t) + \epsilon_2 I_2(t) \\ &\quad - \left[t \left(\frac{b_0\alpha_1^2}{m+b_0b_1} - \alpha_1\epsilon_1 - \frac{\delta b_0\alpha_1\alpha_2}{m+b_0b_1} \right) - \frac{3}{2}\alpha_1 l_1 \right] (w_x^1(l_1, t))^2 \\ &\quad - \left[t \left(\frac{b_0\alpha_2^2}{m+b_0b_1} + \alpha_2\epsilon_2 - \frac{b_0\alpha_1\alpha_2}{\delta(m+b_0b_1)} \right) - \frac{3}{2}\alpha_2(l_2-l_1) \right] (w_x^2(l_1, t))^2 \\ &\quad - \left[t \left(\frac{mb_1}{m+b_0b_1} - \epsilon_1\rho_1 \right) - \frac{3}{2}\rho_1 l_1 \right] (z_t(t))^2 \\ &\quad - \left[t \left(d_1 - \epsilon_2 \left(\frac{d_1^2}{\alpha_2} + \rho_2 \right) \right) - \frac{3}{2}\rho_2(l_2-l_1) \right] (w_t^2(l_2, t))^2. \end{aligned}$$

To ensure nonpositivity, we introduce additional buffer terms in the inequalities

$$\begin{aligned} \frac{dV(t)}{dt} \leq & - \left[tA_1 - \frac{3}{2}\alpha_1 l_1 - \frac{2b_0^2\alpha_1^2}{m+b_0b_1} \right] (w_x^1(l_1, t))^2 \\ & - \left[tA_2 - \frac{3}{2}\alpha_2(l_2-l_1) - \frac{2b_0^2\alpha_2^2}{m+b_0b_1} \right] (w_x^2(l_1, t))^2 \\ & - \left[tA_3 - \frac{3}{2}\rho_1 l_1 - \frac{m^2}{m+b_0b_1} \right] (z_t(t))^2 \\ & - \left[tA_4 - \frac{3}{2}\rho_2(l_2-l_1) \right] (w_t^2(l_2, t))^2, \end{aligned}$$

where A_1, A_2, A_3 , and A_4 are the coefficients inside the time-multiplied terms. Under the assumption $t > \max(T_1, T_2, T_3, T_4)$ from Theorem 6, each bracketed term is positive, hence $\frac{dV(t)}{dt} \leq 0$ for all $t \geq T$. \square

Theorem 7. Assume that the positive constants $\delta, \epsilon_1, \epsilon_2$ satisfy the conditions stated in Theorem 6. Then, there exist constants $M, \sigma > 0$ such that the total energy (7) satisfies the exponential decay estimate:

$$E(t) \leq M e^{-\sigma t} E(0), \quad \forall t > 0. \quad (18)$$

Proof. By Lemma 4, for all $t > T$, we have $(t - C_2)L(t) \leq V(t) \leq V(T) \leq (T + C_2)L(0)$, which implies $L(t) \leq \frac{T+C_2}{t-C_2} L(0)$. Combining this with Lemma 3, we deduce:

$$E(t) \leq \frac{L(t)}{1-2\epsilon C} \leq \frac{1+2\epsilon C}{1-2\epsilon C} \frac{T+C_2}{t-C_2} E(0). \quad (19)$$

Therefore, there exists a time $T^* > T$ and a constant $0 < \zeta < 1$ such that $E(t) \leq \zeta E(0)$ for all $t > T^*$. The exponential decay estimate (18) then follows by standard semigroup arguments. \square

Before the main result, we note that the main challenge is the coupling at the interior mass. The interface variable $\eta(t)$ allows us to capture this in the Lyapunov analysis. Exponential decay is shown even without the lower-order damping b_1 , via a compactness argument.

Theorem 8. Consider the system (1)–(3) with $b_0, d_1 > 0$ and $b_1 = 0$. Then, there exist constants $\tilde{M}, \tilde{\sigma} > 0$ such that the total energy (7) satisfies

$$E(t) \leq \tilde{M} e^{-\tilde{\sigma} t} E(0), \quad \forall t > 0. \quad (20)$$

Sketch of the Proof. Theorem 7 establishes exponential stability when $b_1 > 0$. Removing b_1 modifies the generator \mathcal{A} by a bounded finite-rank perturbation, as the damping $b_1 w_t^1(l_1, t)$ is localized. Hence, $\mathcal{A}|_{b_1=0}$ is a compact perturbation of \mathcal{A} . By [20, Theorem 3.2], exponential stability carries over, yielding (20). \square

IV. A NUMERICAL IMPLEMENTATION

To validate the theory, we run simulations under four damping setups, varying the feedback gains b_0, b_1 , and d_1 to isolate the effects of higher-order, lower-order, and boundary damping. We use $\rho_1 = \sqrt{7}$, $\rho_2 = \pi$, $\alpha_1 = \sqrt{3}$, $\alpha_2 = 1$, $m = 0.6$, $b_0 = b_1 = d_1 = 1$, with $l_1 = 1$ and $l_2 = 2$, reflecting heterogeneity and highlighting damping influence. Simulations assess both the system's spectral properties and its long-time behavior over a fixed horizon.

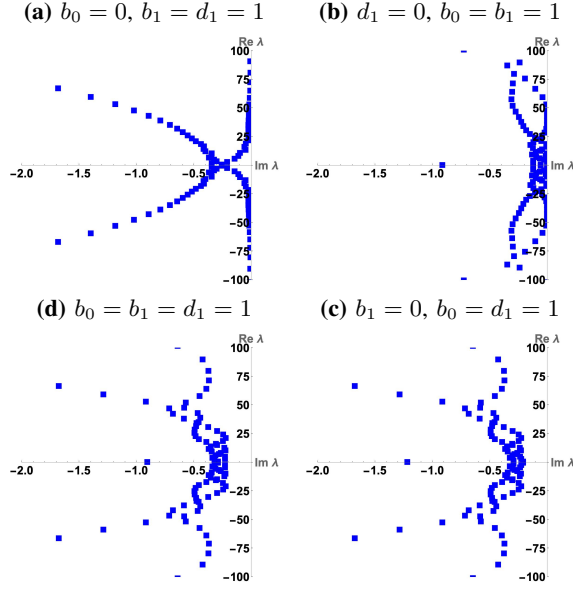


Fig. 2: Eigenvalue distributions of the discrete system matrix A_h under four damping configurations. Subfigures (a)–(d) illustrate how different combinations of the feedback gains b_0 , b_1 , and d_1 affect the spectral placement of eigenvalues and the resulting system stability.

Following [21], let $N_1, N_2 \in \mathbb{N}$ with step sizes $h_1 = \frac{l_1}{N_1+1}$, $h_2 = \frac{l_2-l_1}{N_2+1}$ to discretize $[0, l_1]$ and $[l_1, l_2]$: $0 = x_0^1 < \dots < x_{N_1+1}^1 = l_1$ and $l_1 = x_0^2 < \dots < x_{N_2+1}^2 = l_2$. Let $x_{j+\frac{1}{2}}^i = (x_{j+1}^i + x_j^i)/2$ be midpoints. Approximating $w^i(x_j^i, t) \approx w_j^i(t)$ for $i = 1, 2$, $j = 0, \dots, N_i + 1$, define $w_{j+\frac{1}{2}}^i := \frac{w_{j+1}^i + w_j^i}{2}$, $\delta_{x,h_i} w_{j+\frac{1}{2}}^i := \frac{w_{j+1}^i - w_j^i}{h_i}$, $\delta_{x,h_i}^2 w_j^i := \frac{w_{j+1}^i - 2w_j^i + w_{j-1}^i}{h_i^2}$. First derivatives at midpoints improve accuracy via symmetric stencils [21].

A semi-discrete approximation of (1)–(3) leads to

$$\begin{cases} \rho_i \frac{w_{j-\frac{1}{2},tt}^i + w_{j+\frac{1}{2},tt}^i}{2} - \alpha_i \delta_{x,h_i}^2 w_j^i = 0, & j = 1, \dots, N_i \\ w_0^1 = 0, w_{N_1+1}^1 = w_0^2(t) = z(t) \\ \alpha_1 \delta_{x,h_1} w_{N_1+\frac{1}{2}}^1 + \rho_1 h_1 \frac{w_{N_1+1,tt}^1 + w_{N_1,tt}^1}{4} - \alpha_2 \delta_{x,h_2} w_{\frac{1}{2}}^2 \\ + \rho_2 h_2 \frac{w_{1,tt}^2 + w_{0,tt}^2}{4} + m w_{N_1+1}^1 = -b_1 w_{N_1+1,t}^1 \\ + b_0 (\alpha_2 \delta_{x,h_2} w_{\frac{1}{2},t}^2 - \alpha_1 \delta_{x,h_1} w_{N_1+\frac{1}{2},t}^1), \\ \alpha_2 \delta_{x,h_2} w_{N_2+\frac{1}{2}}^2 + \rho_2 h_2 \frac{w_{N_2+1,tt}^2 + w_{N_2,tt}^2}{4} = -d_1 w_{N_2+1,t}^2 \\ [w_j^i, w_{j,t}^i](0) = (w_0^i, w_1^i)(x_j^i, 0), \quad i = 1, 2. \end{cases} \quad (21)$$

Let $\vec{\Phi} = [w_1^1, \dots, w_{N_1+1}^1, w_1^2, \dots, w_{N_2+1}^2]^\top$ and $\vec{\Psi} := [\vec{\Phi}, \vec{\Phi}_t]^\top$. The discretized system above can be written compactly as $\vec{\Psi}_t = A_h \vec{\Psi}$ where A_h is the system matrix.

For illustration, we set $N_1 = N_2 = 30$. Figure 2 shows the eigenvalue distributions of A_h under four damping configurations. In subfigures (a) and (b), where $b_0 = 0$ or $d_1 = 0$, eigenvalues cluster near the imaginary axis, indicating polynomial decay [12], [15], [16]. In contrast, (c) and (d) show uniform spectral separation when $b_0, d_1 > 0$, confirming exponential decay even without b_1 . This highlights that higher-order and boundary damping alone suffice for exponential stability, refining earlier results that required lower-order damping.

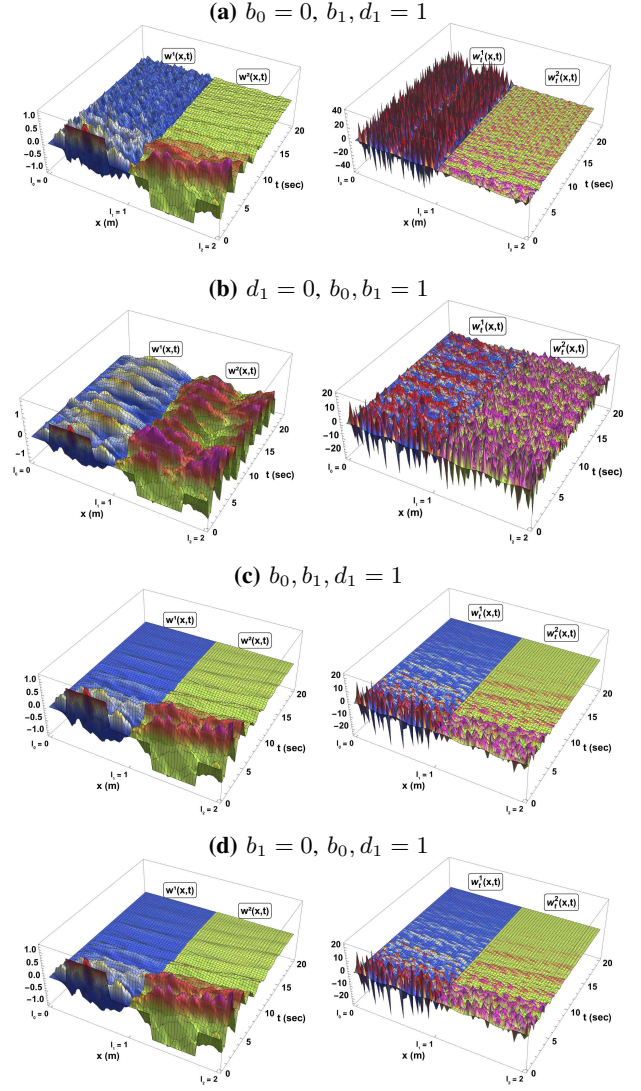


Fig. 3: Time evolution of the displacement fields $\{w^1(x, t), w^2(x, t)\}$ (left column) and their time derivatives $\{w_t^1(x, t), w_t^2(x, t)\}$ (right column) over a 20-second interval. Each row is labeled (a)–(d) and corresponds to a distinct damping configuration as indicated above.

A. A Numerical Experiment

To complement the spectral analysis in Fig. 2, we present time-domain simulations over a 20-second horizon under the same four damping configurations. These simulations visualize the decay of displacement and velocity fields and confirm the theoretical predictions. To assess robustness, we consider sinusoidal (continuous) and box-type (discontinuous) initial conditions. For $i = 1, 2$, we set $w_1^i(x) = \sin\left(\frac{4\pi x}{l_2}\right)$, and $w_0^i(x) = (-1)^{i+1} \chi_{I_i}(x)$, where $I_i := \left(\frac{l_i - l_{i-1}}{2} - \frac{l_i - l_{i-1}}{4}, \frac{l_i - l_{i-1}}{2} + \frac{l_i - l_{i-1}}{4}\right)$ and χ_{I_i} is the characteristic function of I_i . These allow us to examine the system's response to both smooth and localized initial data, highlighting the effectiveness of the damping configuration across varying excitation profiles.

Figure 3 shows the time evolution of the displacement fields $w^1(x, t)$ and $w^2(x, t)$ over a 20-second interval for the

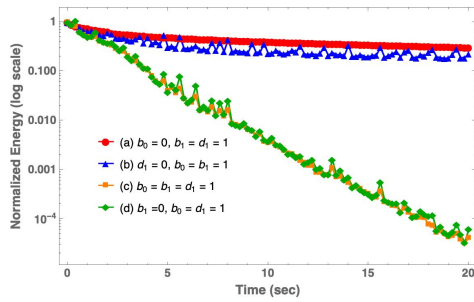


Fig. 4: Normalized energy decay (log scale) over 20 seconds for damping configurations (a)–(d). Cases (a) and (b), lacking b_0 or d_1 , show polynomial decay. Cases (c) and (d) confirm exponential decay, highlighting the role of higher-order and boundary damping.

four damping configurations (a)–(d). Figure 4 displays the corresponding normalized energy decay.

The numerical scheme, based on averaged Finite Differences, was recently developed for this coupled PDE–ODE model [21] and is intentionally kept simple and explicit to ensure clarity and reproducibility; see also [22]. It reliably captures long-time energy behavior and highlights the distinct effects of each damping configuration.

Configurations (a) and (b), with $b_0 = 0$ or $d_1 = 0$, lead to slow, non-exponential decay, confirming that isolated or lower-order damping is inadequate, consistent with Figure 2. Configuration (c), with all damping active, achieves rapid exponential decay (Theorem 7). Configuration (d), with $b_1 = 0$, still yields exponential decay, showing that b_0 and d_1 suffice (Theorem 8). These results show effective stabilization is driven by boundary and higher-order damping.

Remark 1. The simulations use $\epsilon_1 = 0.07087$, $\epsilon_2 = 0.12073$ (within Theorem 6 bounds), and $\delta = 1.53515$, yielding $T = \max(T_1, T_2, T_3, T_4) = 70.22$. Yet, stabilization occurs within 20 seconds, confirming the control’s efficiency.

V. CONCLUSIONS & FUTURE WORK

We prove exponential stability for two strings joined by a dynamic interior mass. Our analysis shows that stability holds without the lower-order damping b_1 , allowing a simpler, more robust design. The result is unconditional, independent of wave speeds or interface location.

A companion study [23] classifies decay rates under six damping scenarios using operator-theoretic tools, covering exponential and polynomial regimes. Future work includes extensions to $k \geq 2$ serially-connected wave equations with multiple interior masses, under partial damping, discontinuous joints [24], and/or sparse actuators. Other challenges include dynamic boundaries, time-delay feedback, and control-matched disturbances, as in [25], [26].

REFERENCES

- [1] J.-M. Coron, *Control and Nonlinearity*, ser. Math. Surveys Monogr. Amer. Math. Soc., 2007, vol. 136.
- [2] J. Wang and M. Krstic, “Vibration suppression for coupled wave pdes in deep-sea construction,” *IEEE Transactions on Control Systems Technology*, vol. 29, no. 4, pp. 1733–1749, 2020.

- [3] F. Di, L. Sun, and L. Chen, “Cable vibration control with internal and external dampers: Theoretical analysis and field test validation,” *Smart Struct. Syst.*, vol. 26, pp. 575–589, 2020.
- [4] K. Ammari, F. Shel, and M. Vanninathan, “Feedback stabilization of a simplified model of fluid–structure interaction on a tree,” *Asymptotic Analysis*, vol. 103, no. 1–2, pp. 33–55, 2017.
- [5] M. A. Bukhari, O. Barry, and E. Tanbour, “On the vibration analysis of power lines with moving dampers,” *Journal of Vibration and Control*, vol. 24, no. 18, pp. 4096–4109, 2018.
- [6] Z. Qiu, C. Li, and X. Zhang, “Experimental study on active vibration control for a kind of two-link flexible manipulator,” *Mech. Systems and Signal Proc.*, vol. 118, pp. 623–644, 2019.
- [7] W. Quan, Q. Chang, Q. Zhang, and J. Gong, “Dynamics calculation for variable-length underwater cable with geometrically nonlinear motion,” *Ocean Engineering*, vol. 212, p. 107695, 2020.
- [8] D. Tsetserukou, R. Tadakuma, H. Kajimoto, N. Kawakami, and S. Tachi, “Variable joint impedance control and development of a whole-sensitive robot arm,” in *Proc. 2007 Int. Symp. on Computational Intelligence in Robotics and Automation*. IEEE, 2007, pp. 338–343.
- [9] G. Chen, M. Coleman, and H. H. West, “Pointwise stabilization in the middle of the span for second-order systems, nonuniform and uniform exponential decay of solutions,” *SIAM Journal on Applied Mathematics*, vol. 47, no. 4, pp. 751–780, 1987.
- [10] E. B. Lee and Y. You, “Stabilization of a vibrating string system linked by point masses,” in *Lecture Notes in Control and Information Sciences*, 1989, pp. 177–198.
- [11] S. Hansen and E. Zuazua, “Exact controllability and stabilization of a vibrating string with an interior point mass,” *SIAM J. on Cont. and Optim.*, vol. 33, no. 5, pp. 1357–1391, 1995.
- [12] W. Littman and S. W. Taylor, *Boundary Feedback Stabilization of a Vibrating String with an Interior Point Mass*. Springer, 2002.
- [13] C. Castro, “Asymptotic analysis and control of a hybrid system composed by two vibrating strings connected by a point mass,” *ESAIM: COCV*, vol. 2, pp. 231–280, 1997.
- [14] K. Ammari, A. Henrot, and M. Tucsnak, “Asymptotic behaviour of the solutions and optimal location of the actuator for the pointwise stabilization of a string,” *Asymptotic Analysis*, vol. 28, no. 3–4, pp. 215–240, 2001.
- [15] S. Avdonin and J. Edward, “Controllability for a string with attached masses and riesz bases for asymmetric spaces,” *Math. Control Relat. Fields*, vol. 9, no. 3, pp. 453–494, 2019.
- [16] J. B. Amara and W. Boughamda, “Exponential stability of two strings under joint damping with variable coefficients,” *Systems & Control Letters*, vol. 141, p. 104709, 2020.
- [17] O. Morgul, B. Rao, and F. Conrad, “On the stabilization of a cable with a tip mass,” *IEEE Transactions on Automatic Control*, vol. 39, no. 10, pp. 2140–2145, 1994.
- [18] B. Guo and C. Xu, “On the spectrum-determined growth condition of a vibration cable with a tip mass,” *IEEE Transactions on Automatic Control*, vol. 45, no. 1, pp. 89–93, 2000.
- [19] M. Krstic and A. Smyshlyaev, “Backstepping boundary control: A tutorial,” in *Proc. Amer. Control Conf.*, 2007, pp. 870–875.
- [20] R. Triggiani, “On the stabilizability problem in banach space,” *J. Math. Anal. Appl.*, vol. 52, no. 2, pp. 383–403, 1975.
- [21] A. Ö. Özer and I. Khalilullah, “Uniformly exponentially stable finite-difference model reduction of heat and piezoelectric beam interactions with static or hybrid feedback controllers,” *Evol. Equ. Control Theory*, vol. 14, no. 2, pp. 339–366, 2025.
- [22] J. Liu and B. Z. Guo, “A new semi-discretized order reduction finite difference scheme for uniform approximation of one-dimensional wave equation,” *SIAM Journal on Control and Optimization*, vol. 58, pp. 2256–2281, 2020.
- [23] M. Akil, Z. Brown, I. Issa, and A. O. Özer, “Dynamic stabilization of two-string systems with interior mass: Unveiling the role of higher-order nodal damping,” 2025, submitted.
- [24] A. Ö. Özer and J. Waltherman, “A uniform observability result for a novel power transmission line model with continuous and discontinuous joints,” in *Proc. Eur. Control Conf.*, Thessaloniki, Greece, 2025.
- [25] Z. D. Mei, “Output feedback exponential stabilization for a one-dimensional wave pde with dynamic boundary,” *J. Math. Anal. Appl.*, vol. 508, no. 1, 2022, paper 125860.
- [26] S. Nicaise and C. Pignotti, “Interior feedback stabilization of wave equations with time dependent delay,” *Electronic Journal of Differential Equations*, vol. 2011, pp. Paper–No. 2011.